

## Discovery of CPI-1612: A Potent, Selective, and Orally Bioavailable EP300/CBP Histone Acetyltransferase (HAT) Inhibitor

Jonathan E Wilson, Gaurav Patel, Chirag Patel, Francois Brucelle, Annissa Huhn, Anna S Gardberg, Florence Poy, Nico Cantone, Archana Bommi-Reddy, Robert J. Sims, Richard T. Cummings, and Julian R. Levell

*ACS Med. Chem. Lett.*, **Just Accepted Manuscript** • DOI: 10.1021/acsmchemlett.0c00155 • Publication Date (Web): 23 Apr 2020

Downloaded from [pubs.acs.org](https://pubs.acs.org) on April 23, 2020

### Just Accepted

“Just Accepted” manuscripts have been peer-reviewed and accepted for publication. They are posted online prior to technical editing, formatting for publication and author proofing. The American Chemical Society provides “Just Accepted” as a service to the research community to expedite the dissemination of scientific material as soon as possible after acceptance. “Just Accepted” manuscripts appear in full in PDF format accompanied by an HTML abstract. “Just Accepted” manuscripts have been fully peer reviewed, but should not be considered the official version of record. They are citable by the Digital Object Identifier (DOI®). “Just Accepted” is an optional service offered to authors. Therefore, the “Just Accepted” Web site may not include all articles that will be published in the journal. After a manuscript is technically edited and formatted, it will be removed from the “Just Accepted” Web site and published as an ASAP article. Note that technical editing may introduce minor changes to the manuscript text and/or graphics which could affect content, and all legal disclaimers and ethical guidelines that apply to the journal pertain. ACS cannot be held responsible for errors or consequences arising from the use of information contained in these “Just Accepted” manuscripts.

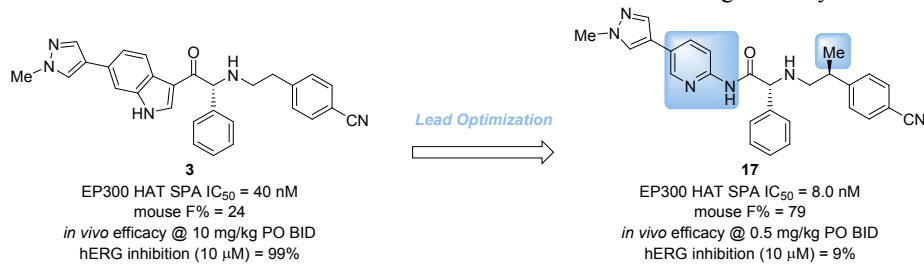
# Discovery of CPI-1612: A Potent, Selective, and Orally Bioavailable EP300/CBP Histone Acetyltransferase (HAT) Inhibitor

Jonathan E. Wilson\*, Gaurav Patel<sup>a</sup>, Chirag Patel<sup>a</sup>, Francois Brucelle<sup>b</sup>, Annessa Huhn<sup>c</sup>, Anna S. Gardberg, Florence Poy, Nico Cantone, Archana Bommi-Reddy, Robert J. Sims III<sup>d</sup>, Richard T. Cummings, Julian R. Levell

Constellation Pharmaceuticals, 215 First Street, Suite 200, Cambridge, MA 02142, United States

**KEYWORDS:** p300, CBP, histone acetyltransferase, HAT, KAT

**ABSTRACT:** The histone acetyltransferases, CBP and EP300, are master transcriptional co-regulators that have been implicated in numerous diseases, such as cancer, inflammatory disorders, and neurodegeneration. A novel, highly potent, orally bioavailable EP300/CBP HAT inhibitor, CPI-1612 or **17**, was developed from the lead compound **3**. Replacement of the indole scaffold of **3** with the aminopyridine scaffold of **17**, led to improvements in potency, solubility, and bioavailability. These characteristics resulted in a 20-fold lower efficacious dose for **17** relative to lead **3** in a JEKO-1 tumor mouse xenograft study.



EP300 and CBP, also known as KAT3A/3B, are two highly homologous, multidomain, epigenetic regulatory enzymes that affect transcription. Although their transcriptional effects are mediated through multiple mechanisms utilizing the different functional domains of these enzymes, the acetylation of histone lysine residues with the cofactor acetyl coenzyme A (AcCoA) by their HAT domains plays a central role in regulating transcription. The HAT domains of EP300 and CBP also modulate the activity of non-histone protein through post-translational acetylation.<sup>1</sup> Both enzymes have been implicated in a wide variety of human diseases, such as cancer, inflammation, fibrosis, and neurodegeneration.<sup>2-7</sup> While loss-of-function in EP300 and/or CBP has been shown to be deleterious, double knockout is lethal in mammals, it has also been shown that overexpression or activating mutations can lead to disease states, particularly in cancer.<sup>8,9</sup> As such, small molecule inhibitors of EP300/CBP HAT activity may provide a novel opportunity for therapeutic intervention in a wide range of human diseases.<sup>10</sup>

We previously described our early drug-discovery efforts towards the identification of leads for the development of novel EP300/CBP HAT inhibitors.<sup>11</sup> With an emphasis on improving the potency of the HTS hit **1**, we independently

explored the SAR of the indole, central benzene, and phenethylamine side chain. To do this, each hydrogen atom of compound **2**, the minimum pharmacophore of lead compound **1**, was replaced with a chlorine atom or methyl group to establish which vectors may allow for introduction of moieties to optimize the potency and physicochemical properties of the scaffold.<sup>12</sup> These efforts culminated in the identification of **3**, a tool compound suitable to validate our biochemical assays, interrogate CBP/EP300 HAT biology *in vitro*, and perform initial *in vivo* experiments. While compound **3** and its analogues were suitable for early proof of concept studies, we sought to improve the potency, oral bioavailability, solubility, and off-target profile of the series with the goal of advancing an EP300/CBP HAT inhibitor into clinical studies. Herein, we describe our medicinal chemistry lead optimization efforts.

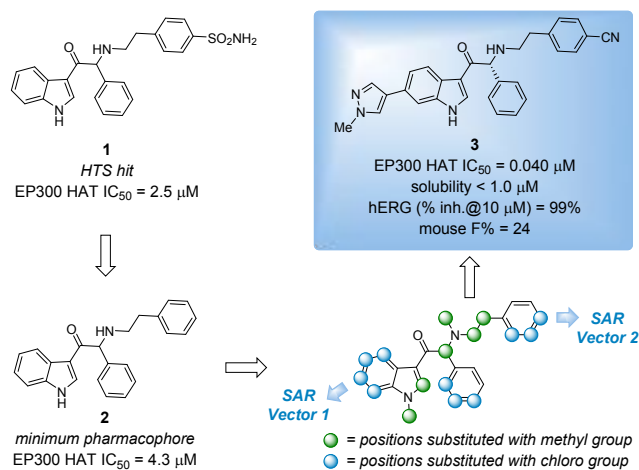


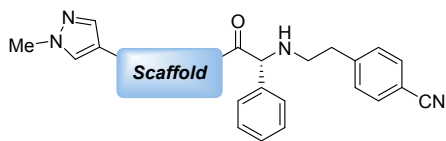
**Figure 1.** Development of lead compound **3** from HTS hit **1**.

The thorough investigation of the SAR outlined in Figure 1 gave us confidence that we had identified the substitution pattern for optimal potency on the phenethylamine side chain, central benzene, and indole core. Subsequently, we focused our attention on the identification of replacements for the indole system, a portion of the molecule that we had not modified up to this stage of the program, that would retain the potency of **3** while improving upon its suboptimal solubility, bioavailability, and hERG inhibition. Our initial efforts in this vein were centered on adding an additional nitrogen atom to the indole core, either in the form of aza-indole **4**, indazole **5** or by substitution with an indole isostere, such as imidazopyridines **6** and **7** or pyrazolopyridine **8**. Only the pyrazolopyridine retained the potency of **3** but with decreased stability in mouse liver microsomes (Table 1). Furthermore, we noted that the potency of compounds **3-8** converged with their respective enantiomers in JEKO-1 cell viability experiments (data not shown). We hypothesized that this convergence in potency was due to compound racemization during the viability assay which was of substantially longer duration relative to the SPA assays.<sup>13</sup> We also sought to address this later issue with future analogues.

The X-ray cocrystal structure of **1** with EP300 led us to hypothesize that the indole of **3** served mainly as a scaffolding element to appropriately position the phenethylamine side chain and the C-6 pyrazole group.<sup>11</sup> This reasoning led us to speculate that a bicyclic scaffold was not required and that it could be replaced with scaffolds that would adopt a conformation in which the benzenoid portion of the indole of **3** was coplanar with its carbonyl group.<sup>14</sup> Based on this reasoning, we chose to explore anilines and amino-heterocyclic amines as replacements for the indole scaffold. While indoline **9** proved to be a potent inhibitor, the compound had poor microsomal stability. The tetrahydroquinoline **10** was not tolerated as a replacement, likely because the tetrahydroquinoline disrupts the coplanar relationship of the scaffold and carbonyl group. While the aniline amide **11** was approximately 3-fold less potent than **3**, it encouraged us to explore additional amino-heterocyclic amides with the hope of identifying a scaffold that would

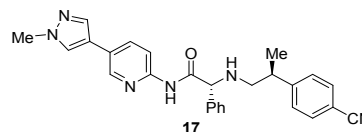
confer improved solubility to this class of inhibitors. This led us to discover the 2-aminopyridine derivative **12**, which possessed improved potency and solubility relative to **3**. Other aminoheterocyclic scaffolds including the regioisomeric pyridine **13**, pyridazine **14**, pyrazine **15**, and pyrimidine **16** were inferior to the 2-aminopyridine **12**.

In addition to its improved potency and solubility, **12** has improved stability to epimerization, permeability and mouse PK relative to **3**. These findings led us to focus our efforts on the optimization of the aminopyridine scaffold. Based on earlier studies examining the effect of substitution of the phenethylamine side chain, a methyl group was incorporated into the phenethylamine side chain of **12** to provide compound **17** with the expectation that it would improve the potency and lower the *in vitro* clearance.<sup>15</sup> Indeed, this modification provided a compound with a 2- to 3-fold improvement in potency across a range of biochemical (EP300 HAT, full length EP300, and full length CBP) and cell-based assays (H3K18Ac MSD and JEKO-1 proliferation) while at the same time improving the microsomal stability. The stereoisomers of **17** were >40-times less potent than **17**.<sup>16</sup> Further modifications to **17** were made, including heterocyclic analogues of the pyrazole, methyl-substituted pyridine analogues, and 2- and 3-fluoro-4-cyanophenethylamine analogues.<sup>17</sup> While some of these analogues provided modest improvements over **17** for a single parameter none of them were better than **17** in aggregate and we focused our attention on **17** for further *in vivo* studies.

**Table 1.** Alternative scaffolds to the indole in compound **3**.

compound	scaffold	EP300 HAT SPA IC <sub>50</sub> (μM) <sup>a</sup>	H3K18Ac MSD EC <sub>50</sub> (μM) <sup>a</sup>	kinetic solubility (μM)	mouse LM clearance (mL/min/kg)
<b>3</b>		0.040 +/- 0.002	0.028 +/- 0.015	<1.0	47
<b>4</b>		0.036 +/- 0.004	NA	NA	NA
<b>5<sup>b</sup></b>		0.57 +/- 0.09	NA	NA	361
<b>6</b>		0.097 +/- 0.009	NA	NA	NA
<b>7</b>		0.52 +/- 0.02	NA	NA	NA
<b>8</b>		0.017 +/- 0.003	NA	<1.0	347
<b>9</b>		0.021 +/- 0.004	NA	2.81	355
<b>10</b>		>5.0	NA	NA	NA
<b>11</b>		0.12 +/- 0.008	NA	<1.0	74
<b>12</b>		0.019 +/- 0.003	0.025 +/- 0.008	23.7	215
<b>13</b>		2.7 +/- 0.2	NA	NA	NA
<b>14</b>		0.46 +/- 0.02	NA	2.96	140
<b>15</b>		0.77 +/- 0.02	NA	NA	NA
<b>16</b>		>5.00	NA	NA	NA

<sup>a</sup>Data is the average of three or more duplicate runs. Error is reported as standard deviation. <sup>b</sup>Compound is racemic.

**Table 2.** Structure of compound **17** and profiles of indole lead **3**, and aminopyridine analogues **12** and **17**.

Compound	<b>3</b>	<b>12</b>	<b>17</b>
<b><i>in vitro</i> assays<sup>a</sup></b>			
EP300 HAT SPA IC <sub>50</sub> (μM)	0.040	0.019	0.0081
Full length EP300 SPA IC <sub>50</sub> (μM)	0.0025	<0.0005	<0.0005
Full length CBP SPA IC <sub>50</sub> (μM)	0.0032	0.0067	0.0029
H3K18Ac MSD EC <sub>50</sub> (μM)	0.037	0.025	0.014
JEKO-1 GI <sub>50</sub> (μM)	0.044	0.017	<0.0079
hERG (% inh. @ 10 μM)	97	n.a.	9.2
PAMPA pe (nm/s)	<0.066	13.8	11.9
Mouse PPB (%)	99.1	98.3	99.1
MLM Cl (μL/min/mg)	46.6	215	178
<b><i>Mouse PK<sup>b</sup></i></b>			
Clearance (L/h/kg)	3.49	2.30	1.88
V <sub>ss</sub> obs	1.92	0.88	0.99
T <sub>1/2</sub> (hours)	1.44	1.24	1.40
F%	43	88	47

<sup>a</sup>All biochemical assays are the average of two or more runs. PAMPA, mouse PPB, and MLM assays are a single run. <sup>b</sup>Mouse PK data are derived from cassette PK experiments, using 0.5 mg/kg IV and 2.5 mg/kg PO doses.

The high EP300 potency, promising *in vitro* profile, and good mouse PK of **17** prompted us to further profile this compound's pharmacokinetic profile in rats and dogs. While the oral exposure of **17** in dogs (0.5 mg/kg IV; 1.0 mg/kg PO; clearance = 0.42 L/h/kg, V<sub>ss</sub> = 3.7 L/kg, T<sub>1/2</sub> = 5.5 h, F% = 71; AUC/dose = 1,691 h\*mg/mL) and mice (1mg/kg IV; 5 mg/kg PO; clearance = 3.8 L/h/kg, V<sub>ss</sub> = 2.0 L/kg, T<sub>1/2</sub> = 0.98 h, F% = 79; AUC/dose = 211 h\*mg/mL) is good, the exposure in rats is limited by poor bioavailability (1.0 mg/kg IV; 5.0 mg/kg PO; clearance = 2.6 L/h/kg, V<sub>ss</sub> = 1.8 L/kg, T<sub>1/2</sub> = 1.2 h, F% = 9; AUC/dose = 35.6 h\*mg/mL).<sup>18</sup> Additionally, because there are many potential indications where a brain-penetrant EP300/CBP HAT inhibitor would of interest, we performed a mouse PK experiment to monitor for brain exposure.<sup>6,7</sup> In this experiment, a single dose of **17** was administered orally to CD-1 mice and brain and plasma exposures of **17** were measured at 0.25, 0.5, 1.0, 2.0, 4.0, and 8.0 hours. **17** is highly brain-penetrant showing a brain-to-plasma ratio of 0.35 after a single oral dose.<sup>19</sup>

Compound **17** was then characterized for its selectivity against other histone acetyltransferases and a panel of typical anti-targets. No inhibitory activity was observed in a panel of 7 HAT targets (Tip60, HAT1, PCAF, MYST2, MYST3, MYST4, and GCN5L2) and had minimal activity against the anti-targets in the Eurofins Safety44 off-target screening panel. Additionally, **17** showed weak activity in a hERG binding assay (IC<sub>50</sub> = 10.4 μM) and displayed

moderate inhibition of CYP2C8 ( $IC_{50} = 1.9 \mu M$ ) and CYP2C19 ( $IC_{50} = 2.7 \mu M$ ) but showed less inhibition of CYP3A4, CYP2D6, CYP1A2, CYP2B6, and CYP2C9 ( $>50 \mu M$ ,  $34 \mu M$ ,  $>50 \mu M$ ,  $8.2 \mu M$ ,  $6.6 \mu M$ ).

X-ray cocrystal structures, obtained utilizing the methodology described by Abbvie, clearly show that compounds **12** and **17** bind to the acetylcoenzyme A binding site.<sup>11</sup> Figure 2 shows an overlay of AcCoA and **12** that highlights the major ligand-protein contacts of **12** to the EP300 HAT domain. Several of the binding interactions are common for indole **1** and aminopyridine **12**. These include the SER1400 H-bonding interaction to the phenethylamine N-H and the  $\pi$ -stacking interactions of TRP1466 to the phenethylamine aromatics and of HIS1451 to the indole of **1** or the aminopyridine of **12**. A key difference between the crystal structures of **1** and **12** that may account for the improved potency of **12** relative to **3**, is a H-bonding network that is established between the aminopyridine of **12** with ASP 1399 and a water bound to the backbone N-H of TYR1446. This water is not found in the co-crystal structure of **1** presumably because it has been displaced by the indole N-H.

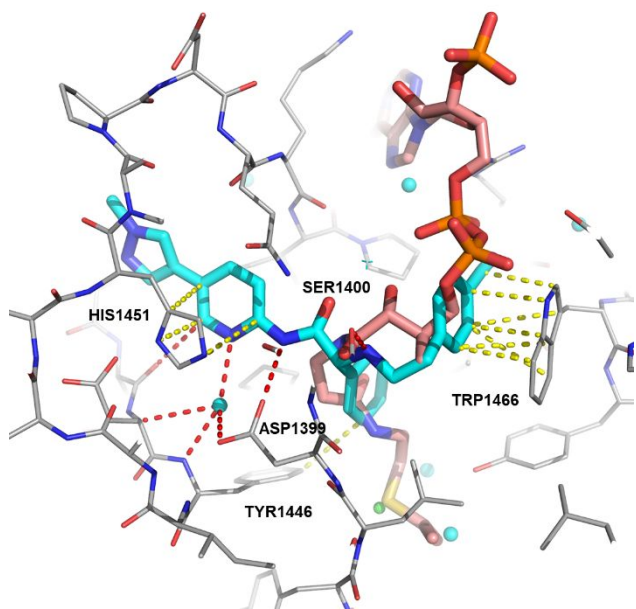


**Figure 2.** Overlay of X-ray cocrystal structures of **12** (cyan) and acetylcoenzyme A (pink) bound to the HAT domain of EP300 with key hydrogen bonds (red) and pi-stacking interactions (yellow) of **12** with EP300 highlighted.

While both our series of inhibitors and Abbvie's occupy the AcCoA pocket of EP300, the contacts the two classes make with the protein are somewhat distinct. While both compounds make hydrogen bonds with SER1400, **17** does so through an N-H bond and A-485 through a carbonyl group from the oxazolidinone.<sup>20, 21</sup> The only other interaction common to both inhibitors is a  $\pi$ -stacking interaction with HIS1451. The other interactions the compounds make with the protein are distinct. A-485 makes two hydrogen bonds from a urea moiety with the backbone carbonyl of GLN1455, while **17** makes no direct contact with this residue. In contrast **17** makes hydrogen

bonds with the backbone N-H of TYR1446 and to ASP1399 through the aminopyridine scaffold, while A-485 makes no direct contact with this residue. Another difference in the binding modes are the interactions of the aromatic side chains. The 4-cyanophenethylamine side chain of **17** interacts with TRP1466 through a  $\pi$ -stacking interaction while the 4-fluorobenzamide of A-485 fills a pocket formed by TYR1414 and LEU1418. This later pocket is filled by the methyl group on the phenethylamine side chain of **17**.

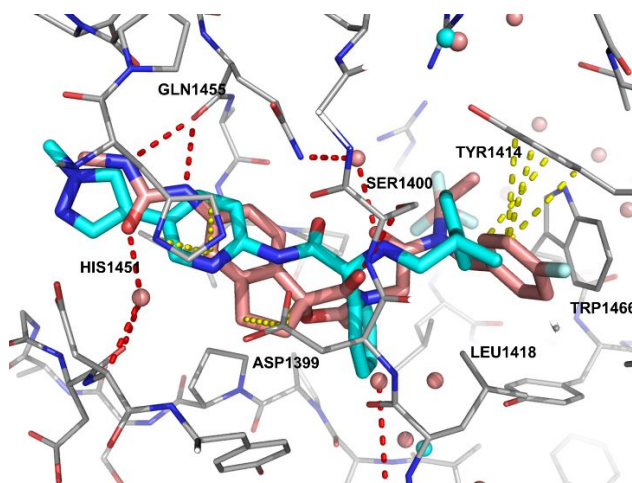


**Figure 3.** Overlay of X-ray cocrystal structures of **17** (cyan) and A-485 (pink) bound to the HAT domain of EP300 with key hydrogen bonds (red) and pi-stacking interactions (yellow) of A-485 highlighted.

The *in vivo* activity of **17** was assessed by conducting a PK/PD study in C57B6 mice, measuring H3K27Ac reduction in PBMCs and H3K18Ac reduction in spleen tissue (data not shown) after oral administration of **17**. As expected, based on its high potency and good pharmacokinetic profile, **17** reduces the histone acetylation *in vivo* at the primary chromatin acetylation targets of EP300/CBP in a dose- and time-dependent manner (Figure 4).

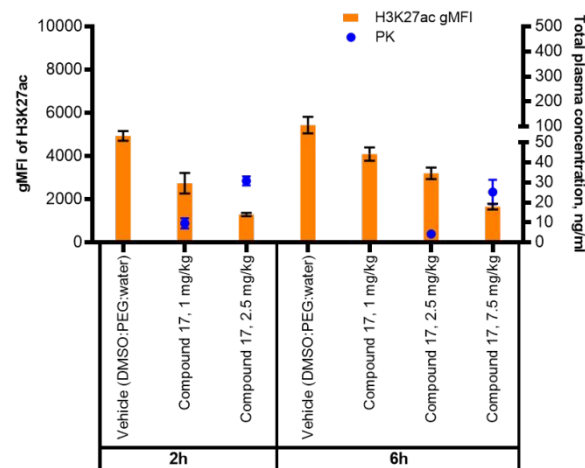


**Figure 4.** Dose- and time-dependent reduction of H3K27Ac in PBMCs of C57Black6 mice after oral administration of compound **17**.

The efficacy of **17** was then assessed in a mouse tumor xenograft model using a B-cell lymphoma line, JEKO-1, which we have shown is sensitive to CBP/EP300 HAT inhibition. **17** showed 67% TGI at a dose of 0.5 mg/kg PO BID with concomitant reduction of H3K27Ac in plasma and reduction of H3K18Ac in the tumor. These effects are approximately equivalent to those observed with **3** when dosed at 10 mg/kg BID PO (65% TGI). This represents a 20-fold improvement of *in vivo* activity for **17** relative to **3**, with an improved off-target profile. This improvement in *in vivo* activity can mainly attributed to the improved potency, permeability, and solubility of **17** relative to **3** (Figure 5).

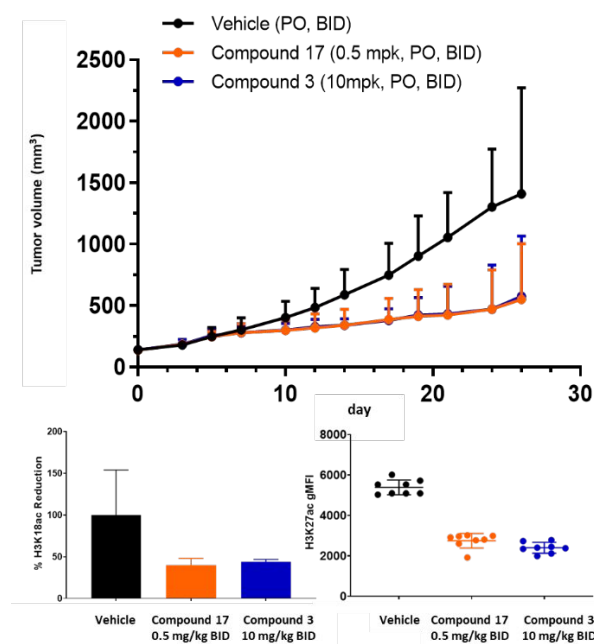


**Figure 5.** Antitumor activity (top), H3K18Ac reduction in tumor (bottom left), and H3K27Ac reduction in plasma (bottom right) of **17** (orange) and **3** (blue) in a JEKO-1 xenograft model.

In summary, we have detailed the optimization of lead indole compound **3** into the highly potent and selective aminopyridine EP300/CBP HAT inhibitor CPI-1612, **17**. A wide variety of scaffold replacements for the indole were surveyed, resulting in the discovery of the aminopyridine core of **12**. Further optimization led us to compound CPI-1612 which is potent across a range of biochemical and cellular assays that assess EP300/CBP HAT inhibition, has good pharmacokinetic profiles in mice and dogs, and is devoid of any significant off-target activity. Additionally, CPI-1612 suppresses H3K27 acetylation *in vivo* and is efficacious in a JEKO-1 mantle cell lymphoma xenograft at a low dose.

## ASSOCIATED CONTENT

### Supporting Information

The Supporting Information is available free of charge on the ACS Publications website.

The preparation of compounds **3-17**, experimental details for *in vivo* experiments and ADME experiments, and details for x-ray crystallography of compounds **12** and **17** are available as a PDF.

The PDB deposition validation reports are also available as a PDF.

## AUTHOR INFORMATION

### Corresponding Author

\* Email: jonathan.wilson@constellationpharma.com

### Present Addresses

<sup>a</sup> Piramal Enterprises Limited-Discovery Solutions  
Ahmedabad, Gujarat, IN 382 213.

<sup>b</sup> Foghorn Therapeutics, 100 Binney Street, Suite 610, Cambridge, MA, USA 02142.

<sup>c</sup> Kymera Therapeutics, 300 Technology Square, Cambridge, MA, USA 02142.

<sup>d</sup> Third Rock Ventures, 29 Newbury St #301, Boston, MA, USA 02116.

### Author Contributions

The manuscript was written through contributions of all authors. / All authors have given approval to the final version of the manuscript.

## ABBREVIATIONS

CBP, CREB binding protein; HAT, histone acetyltransferase; AcCoA, acetyl coenzyme A; H3K27, histone 3 lysine 27; H3K18, histone 3 lysine 18; HTS, high throughput screen; SAR, structure activity relationship; SPA, scintillation proximity assay; MSD, meso scale discovery; PAMPA, parallel artificial membrane permeation assay; PPB, plasma protein binding; MLM, mouse liver microsomes; PK, pharmacokinetics; hERG, human ether- $\alpha$ -go-go-related gene or K<sub>v</sub> 11.1; IV, intravenous; PO, per os; TGI, tumor growth inhibition.

## REFERENCES

- (1) Dancy, B. M.; Cole, P. A. Protein Lysine Acetylation by p300/CBP. *Chem. Rev.* **2015**, *115*, 2419-2452.
- (2) Attar, N.; Kurdistani, S. K. Exploitation of EP300 and CREBBP Lysine Acetyltransferases by Cancer. *Cold Spring Harbor Perspect. Med.* **2017**, *7*, a026534.
- (3) Farria, A.; Li, W.; Dent, S. Y. R. KATs in Cancer: Functions and Therapies. *Oncogene* **2015**, *34*, 4901-4913.
- (4) Ghosh, A. K.; Varga, J. The Transcriptional Coactivator and Acetyltransferase p300 in Fibroblast Biology and Fibrosis. *J. Cellular Physiology* **2007**, *12*, 663-671.
- (5) Ghizzoni, M.; Haisma, H. J.; Maarsingh, H.; Dekker, F. J. Histone acetyltransferases are crucial regulators in NF- $\kappa$ B mediated inflammation. *Drug Discovery Today* **2011**, *16*, 504-511.
- (6) Valor, L. M.; Viosca, J.; Lopez-Atalaya, J. P.; Barco, A. Lysine Acetyltransferases CBP and p300 as Therapeutic Targets in Cognitive and Neurodegenerative Disorders. *Current Pharmaceutical Design* **2013**, *19*, 5051-5064.
- (7) Min, S.-W.; Chen, X.; Tracy, T. E.; Li, Y.; Zhou, Y.; Wang, C.; Shirakawa, K.; Minami, S. S.; Defensor, E.; Mok, S. A.; Sohn, P. D. M.; Schilling, B.; Cong, X.; Ellerby, L.; Gibson, B. W.; Johnson, J.; Krogan, N.; Shamloo, M.; Gestwicki, J.; Masliah, E.; Verdin, E.; Gan, L. Critical role of acetylation in tau-mediated neurodegeneration and cognitive deficit. *Nature Medicine* **2015**, *21*, 1154-1162.
- (8) Tanaka, Y.; Naruse, I.; Maekawa, T.; Masuya, H.; Shiroishi, T.; Ishii, S. Abnormal skeletal patterning in embryos lacking a single Cbp allele: A partial similarity with Rubinstein-Taybi syndrome. *Proc. Natl. Acad. Sci. U.S.A.* **1997**, *94*, 10215-10220.
- (9) Yao, T. P.; Oh, S. P.; Fuchs, M.; Zhou, N. D.; Ch'ng, L. E.; Newsome, D.; Bronson, R. T.; Li, E.; Livingston, D. M.; Eckner, R. Gene Dosage-Dependent Embryonic Development and Proliferation Defects in Mice Lacking the Transcriptional Integrator p300. *Cell* **1998**, *93*, 361-372.

(10) Lasko, L.M.; Jakob, C.S.; Edalji, R.P.; Qiu, W.; Montgomery, D.; Digiammarino, E. L.; Hansen, T. M.; Risi, R. M.; Frey, R.; Manaves, V.; Shaw, B.; Algire, M.; Hessler, P.; Lam, L. T.; Uziel, T.; Faivre, E.; Ferguson, D.; Buchanan, F. G.; Martin, R. L.; Torrent, M.; Chiang, G. G.; Karukurichi, K.; Langston, J. W.; Weinert, B. T.; Choudhary, C.; DeVries, P.; VanDrie, J.H. ;McElligott,D.;Kesicki, E.; Marmorstein, R.; Sun, C.; Cole, P. A.; Rosenberg, S.; Michaelides, M. R.; Lai, A.; Bromberg, K. D. Discovery of a selective catalytic p300/CBP inhibitor that targets lineage-specific tumors. *Nature* **2017**, *550*, 128–132.

(11) Wilson, J. E.; Huhn, A.; Gardberg, A. S.; Poy, F.; Brucelle, F.; Vivat, V.; Patel, G.; Patel, C.; Cummings, R; Sims, R.; Levell, J.; Audia, J. E.; Bommi-Reddy, A.; Cantone, N. Early Drug Discovery Efforts Towards the Identification of EP300/CBP Histone Acetyltransferase (HAT) Inhibitors. *ChemMedChem* **2020**, doi.org/10.1002/cmdc.202000007.

(12) Data for chlorine- and nitrogen-‘walk’ studies can be found in the associated supporting information document for reference 11.

(13) The EP300 HAT SPA enzymatic assay was run for 1 hour while the JEKO-1 cell viability assay was run for 72 hours.

(14) The x-ray cocrystal structure of **1** clearly shows that the indole scaffold and the 3-carbonyl group are coplanar. The x-ray structure of **1** with an EP300 HAT construct has been deposited in the PDB (6v8b). See reference 11.

(15) In all cases we have examined, addition of a methyl group at the carbon atom adjacent to the aromatic group that is part of the phenethylamine side chain provides approximately a 2- to 3-fold improvement in potency in the EP300 HAT domain SPA assay. See the supporting information for additional data.

(16) See the supporting information for additional information.

(17) Wilson, J. E.; Brucelle, F.; Levell, J. R. Amino amides as P300/CBP HAT inhibitors and their preparation. Pat. Appl. WO2019161162.

(18) The data in the text are for single compound PK experiments with **17** while those in Table 3 are experiments with a cassette of at least 3 compounds each. For comparison the single compound mouse PK for compound **3** is as follows: 1mg/kg IV; 10 mg/kg PO; clearance = 3.0 L/h/kg, V<sub>ss</sub> = 1.9 L/kg, T<sub>1/2</sub> = 0.98 h, F% = 26; AUC/dose = 90 h\*mg/mL.

(19) Compound **17** was administered orally to eighteen male CD-1 mice. Plasma, brain, and CSF levels of compound **17** were then determined at multiple time points. See the supporting information for experimental details and additional data.

(20) Michaelides, M. R.; Kluge, A.; Patane, M.; Van Drie, J. H.; Wang, C.; Hansen, T. M.; Risi, R. M.; Mantei, R.; Hertel, C.; Karukurichi, K.; Nesterov, A.; McElligott, F.; de Vries, P.; J. William Langston, J. W.; Cole, P. A.; Marmorstein, R.; Liu, H.; Lasko, L.; Bromberg, K. D.; Lai, A.; Kesick, E. A. Discovery of Spiro Oxazolidinediones as Selective, Orally Bioavailable Inhibitors of p300/CBP Histone Acetyltransferases. *ACS Med. Chem. Lett.* **2018**, *9*, 28-33.

(21) The structure of A-485 is shown below.

